



# SMARCC1 Suppresses Tumor Progression by Inhibiting the PI3K/AKT Signaling Pathway in Prostate Cancer

## OPEN ACCESS

### Edited by:

Yongbin Chen,  
Kunming Institute of Zoology (CAS),  
China

### Reviewed by:

Huiqing Wang,  
Second Military Medical University,  
China

Zhifeng Liu,

General Hospital of Guangzhou  
Military Command, China

Zhijie Li,

Jinan University, China

### \*Correspondence:

Shan-Chao Zhao  
lulululu@smu.edu.cn

†These authors have contributed  
equally to this work and share first  
authorship

### Specialty section:

This article was submitted to  
Molecular and Cellular Oncology,  
a section of the journal  
Frontiers in Cell and Developmental  
Biology

Received: 10 March 2021

Accepted: 16 April 2021

Published: 25 June 2021

### Citation:

Xiao Z-M, Lv D-J, Yu Y-z, Wang C,  
Xie T, Wang T, Song X-L and  
Zhao S-C (2021) SMARCC1  
Suppresses Tumor Progression by  
Inhibiting the PI3K/AKT Signaling  
Pathway in Prostate Cancer.  
Front. Cell Dev. Biol. 9:678967.  
doi: 10.3389/fcell.2021.678967

Zhao-Ming Xiao<sup>1†</sup>, Dao-Jun Lv<sup>2†</sup>, Yu-zhong Yu<sup>1</sup>, Chong Wang<sup>1</sup>, Tao Xie<sup>1</sup>, Tao Wang<sup>1</sup>,  
Xian-Lu Song<sup>3</sup> and Shan-Chao Zhao<sup>1,4\*</sup>

<sup>1</sup> Department of Urology, Nanfang Hospital, Southern Medical University, Guangzhou, China, <sup>2</sup> Guangdong Key Laboratory of Urology, Department of Urology, Minimally Invasive Surgery Center, The First Affiliated Hospital of Guangzhou Medical University, Guangzhou, China, <sup>3</sup> Department of Radiotherapy, Affiliated Cancer Hospital and Institute of Guangzhou Medical University, Guangzhou, China, <sup>4</sup> Department of Urology, The Third Affiliated Hospital, Southern Medical University, Guangzhou, China

**Background:** SWI/SNF-related, matrix-associated, actin-dependent regulator of chromatin subfamily C member 1 (*SMARCC1*) protein is a potential tumor suppressor in various cancers. However, its role in prostate cancer (PCa) remains controversial. The aim of this study was to determine the biological function of *SMARCC1* in PCa and explore the underlying regulatory mechanisms.

**Methods:** The expression of *SMARCC1* was validated in PCa tissues by immunohistochemistry. Meanwhile, function experiments were used to evaluate the regulatory role on cell proliferation and metastasis in PCa cells with *SMARCC1* depletion both *in vitro* and *in vivo*. The expression levels of relevant proteins were detected by Western blotting.

**Results:** Our finding showed that *SMARCC1* was significantly downregulated in prostate adenocarcinoma, with a higher Gleason score (GS) than that in low GS. The decreased expression of *SMARCC1* was significantly correlated with a higher GS and poor prognosis. Additionally, we found that silencing of *SMARCC1* dramatically accelerated cell proliferation by promoting cell cycle progression and enhancing cell migration by inducing epithelial mesenchymal transition (EMT). Furthermore, depletion of *SMARCC1* facilitated PCa xenograft growth and lung metastasis in murine models. Mechanistically, the loss of *SMARCC1* activated the *PI3K/AKT* pathway in PCa cells.

**Conclusion:** *SMARCC1* suppresses PCa cell proliferation and metastasis *via* the *PI3K/AKT* signaling pathway and is a novel therapeutic target.

**Keywords:** *SMARCC1*, prostate cancer, proliferation, epithelial-mesenchymal-transition, *PI3K/AKT* pathway

## INTRODUCTION

Prostate cancer (PCa) is a common malignancy afflicting elderly males, with over 1.6 million men diagnosed every year (Pernar et al., 2018; Siegel et al., 2021). In America, the morbidity rate of PCa has ranked first in all cancer-related deaths (Siegel et al., 2021). Globally, it is estimated that 366,000 men die of PCa annually, making it the fifth most common cause of cancer-related deaths worldwide (Pernar et al., 2018; Siegel et al., 2021). Multiple mutations in several key epigenetic factors, including Rb1 and BRCA, drive the progression of PCa to aggressive phenotype at terminal stage, characterized by limited survival, revealing an important role of epigenetic dysregulation on PCa progression (Crea et al., 2011; Liu, 2016; Chan et al., 2018; Sheahan and Ellis, 2018; Oh et al., 2019; Wu et al., 2019; Ge et al., 2020; Liang et al., 2020). However, the specific function and profound mechanisms of various epigenetic factors involved in PCa progression are still uncertain. Thus, it is extremely urgent and worthwhile to further explore the role and mechanisms of epigenetic regulators in PCa progression.

The SWI/SNF-related, matrix-associated, actin-dependent regulator of chromatin subfamily C member 1 (SMARCC1) is one of the core subunits of the SWI/SNF complex involved in epigenetic regulation on genome transcription (Reisman et al., 2009; Shain and Pollack, 2013; Hohmann and Vakoc, 2014; Alver et al., 2017; Lu and Allis, 2017; Savas and Skardasi, 2018). It is regarded as a tumor suppressor in several cancers, including renal, colon, and pancreatic carcinoma (Andersen et al., 2009; Iwagami et al., 2013; Wang et al., 2021). However, its role in PCa remains ambiguous and controversial. Previous studies have shown that SMARCC1 is upregulated in PCa tissue and may promote the initiation and progression in PCa *via* the transactivating androgen receptor (Hong et al., 2005; Heebøll et al., 2008), whereas a retrospective study on patients with local PCa indicated that SMARCC1 positive staining in the prostate biopsy samples correlated with prolonged survival, which is indicative of a tumor-suppressive role in PCa (Hansen et al., 2011). These discrepancies may be partly attributed to different cancer models and expression systems.

In this study, we aimed to explore the role of SMARCC1 in the proliferation and metastasis of PCa by using a series of *in vitro* functional assays and *in vivo* mouse model due to lack of conclusive research on the mechanism of SMARCC1 during PCa progression. Moreover, the potential mechanism by which

SMARCC1 mediates the development and progression of PCa was also investigated.

## MATERIALS AND METHODS

### Prostate Cancer Tissues

Tumor and matched benign prostatic hyperplasia tissue samples were collected from 100 PCa patients who received radical prostatectomy for prostate cancer at Nanfang Hospital, Southern Medical University (Guangzhou, China). The PCa patients were enrolled in our research project according to the following standards: (1) the patients were diagnosed with PCa before surgery, in accordance with biopsy pathological diagnosis, (2) post-operation pathological examination confirmed the diagnosis of PCa, and (3) the patients were informed and consented to the collection of specimens. Meanwhile, some PCa patients were excluded from our research cohort due to the following criteria: (1) patients with other malignant diseases or a second primary tumor, (2) PCa patients who received preoperative androgen deprivation therapy, chemotherapy, or radiotherapy before surgery, and (3) HIV- or syphilis-positive patients. The relevant clinicopathological data of the patients was also obtained. All patients signed the informed consent, and sample collection was approved by the ethical protocols of the Ethics Committee of Nanfang Hospital, Southern Medical University.

### Immunohistochemistry

The paraffin sections were dewaxed in xylene, rehydrated through an ethanol gradient, and washed in phosphate buffer saline (PBS). After boiling in 10 mM citrate buffer (pH 6) for 10 min for antigen retrieval, the sections were immersed in 3% H<sub>2</sub>O<sub>2</sub> for 10 min to inhibit endogenous peroxidase. The sections were then blocked with 1% goat serum and incubated overnight with primary antibodies against SMARCC1 (1:800; Abcam, cat. ab126180, United States), E-Cadherin (1:100; CST, cat. 24E10, United States), *Claudin1* (1:100; CST, cat. 13255T, United States), MMP2 (1:50; HuaBio, cat. ER40806, China), *P504S* (1:100; Proteintech, cat. 15918-1-AP, China), and *Ki67* (1:100; Biossci, cat. BA1063, China) at 4°C. After washing thrice with PBS, the sections were then probed with the secondary antibody for 1 h and rinsed three times with PBS. The DAB Kit (Biossci, cat. BP0770, China) was used for immunostaining, and the nucleus was counterstained with hematoxylin. The sections were then dehydrated through an ethanol gradient and sealed with neutral balsam. The stained sections were observed under a light microscope (BX53, Olympus, Japan) fitted with a digital camera (DP72, Olympus, Japan). The *in situ* SMARCC1 expression level was analyzed independently by two pathologists blinded to the patients' clinical information. The staining intensity was scored as negative (0), weak (1), medium (2), or strong (3), and the percentage of positively stained area was scored as 0 (0%), 1 (1–25%), 2 (26–50%), 3 (51–75%), and 4 (76–100%). The total staining score was calculated by multiplying the intensity and positivity scores, and the samples were graded as low (0–5), medium (6–8), and high (9–12) expression accordingly. In addition, low staining intensity in tissue was classified as

**Abbreviations:** PCa, prostate cancer; SMARCC1, SWI/SNF-related, matrix-associated, actin-dependent regulator of chromatin subfamily C member 1; BPH, benign prostatic hyperplasia; GS, Gleason score; SWI/SNF complex, Switch/sucrose non-fermentable complex; H&E staining, hematoxylin and eosin staining; PSB, phosphate buffer solution; siRNA, small interference RNA; shRNA, short hairpin RNA; MOI, multiplicity of infection, qRT-PCR, quantitative real-time polymerase chain reaction; cDNA, complementary DNA; GAPDH, glyceraldehyde-3 phosphate dehydrogenase; RIPA, radio-immunoprecipitation assays; PMSE, phenylmethylsulfonyl fluoride solution; SDS-PAGE, sodium dodecyl sulfate polyacrylamide gel electrophoresis; PVDF, polyvinylidene fluoride; HRP, horseradish peroxidase; DMSO, dimethyl sulfoxide; SEM, standard error of mean; CDK, cyclin-dependent kinase; CKI, cyclin-dependent kinase inhibitor; EMT, epithelial to mesenchymal transition; MMP2, matrix metalloproteinase 2; PBST, PBS-tween solution; PI3K/AKT, phosphatidylinositol 3 kinase/protein kinase B; Rb1, retinoblastoma-associated protein 1; BRCA, breast cancer susceptibility gene; ATPase, adenosine triphosphatase.

negative, while both medium and high staining intensity were classified as positive.

## Bioinformatics Analyses

The disease-free survival data was extracted from the Gene Expression Profiling Interactive Analysis (GEPIA) database<sup>1</sup> and analyzed using R. The cutoff was set as 30% high vs. 70% low.

## Cell Culture

RWPE-1, LNCAP, C4-2, PC3, 22RV1, and DU145 cell lines were obtained from the Cell Bank of Typical Culture Preservation Committee of the Chinese Academy of Sciences (Shanghai, China). The RWPE-1 cells were cultured in primary keratinocyte culture medium (iCell Bioscience Inc., cat. PriMed-iCell-010, China), and the other cell lines were cultured in RPMI 1640 (Gibco, cat. 11875-093, United States) supplemented with 10% fetal bovine serum (FBS; Gibco, cat. 10270-106, United States) and 1% penicillin–streptomycin solution (Gibco, 15140-122, United States) at 37°C under 5% CO<sub>2</sub>. As per experimental requirements, the cells were treated with 20 ng/ml LY294002 (Macklin, cat. HY-10108, China) in dimethyl sulfoxide for 24 h (Bao et al., 2015).

## SMARCC1 Knockdown

The cells were seeded in six-well plates at a density of  $0.5 \times 10^6$  cells/well and transfected 24 h later with *SMARCC1* siRNA using Lipofectamine 3000 (Invitrogen, United States). The cells were harvested 48 h after transfection, and *SMARCC1* mRNA and protein levels were analyzed by quantitative real-time polymerase chain reaction (qRT-PCR) and western blotting. The lentivirus vector containing the *SMARCC1* shRNA was synthesized by Vigene Biosciences Inc. (China). Briefly,  $0.5 \times 10^6$  cells were plated in six-well plates and infected 24 h later with the virus at a multiplicity of infection (MOI) of 30 in serum-free medium. Fresh complete medium containing 2 µg/ml puromycin was added 48 h after transfection, and the cells were cultured for 4 days. The sh-*SMARCC1* cell lines with stable knockdown were detected by qRT-PCR and western blotting. siRNA targeted to *SMARCC1*: 5'-CCUCACAAGACGAUGAAGATT-3' 5'-UCUUCAUCGUCUUGUGAGGTT-3' was synthesized in GenePharma Co., Ltd (Suzhou, CHINA) and sh RNA contained in lentivirus vectors was designed according to siRNA sequence.

## RNA Extraction and qRT-PCR

RNA was extracted using Trizol reagent (Invitrogen, cat. 15596018, United States) and reverse-transcribed to cDNA using PrimeScript RT Master Mix Kit (Takara, cat. RR036A, Japan) according to the manufacturer's instructions. The cDNA was amplified with the PrimeScript<sup>TM</sup> RT-PCR Kit (Takara, cat. DRR015A, Japan) on Applied Biosystems<sup>TM</sup> 7500 fast Dx real-time PCR cyler (ThermoFisher, United States) according to the manufacturer's protocol. GAPDH was used as the internal control, and relative expression levels were calculated by the  $2^{-\Delta\Delta CT}$  method. Primer sequence was obtained from website primerbank (<https://pga.mgh.harvard.edu/primerbank/>) and shown as following: *SMARCC1* (Forward sequence:

5'-AGCTGTTTATCGACGGAAGGA-3'; Reverse sequence: 5'-GCATCCGCATGAACATACTTCTT-3'); GAPDH (Forward sequence: 5'-GGAGCGAGATCCCTCCAAAAT-3'; Reverse sequence: 5'-GGCTGTTGTCATACTTCTCATGG-3').

## Protein Extraction and Western Blotting

The suitably treated cells were homogenized in radio-immunoprecipitation assay (RIPA) buffer supplemented with phenylmethylsulfonyl fluoride (KGP250, KeyGEN BioTECH, Nanjing, China) at the ratio of 1,000:1, along with protease inhibitor (Mecklin, cat. P885281, China) and phosphatase inhibitor (FDbio, cat. FD7186, China), each at 100:1 ratio. The cells were lysed by ultrasonication for 20 min and centrifuged at 12,000 rpm for 5 min at 4°C. The nuclear and cytoplasmic proteins were fractionated using the nucleus extraction kit (Pythonbio, cat. AAPR285, Guangzhou, China). Briefly,  $1 \times 10^7$  of cells were lysed using a specific buffer at 4°C for 20 min and centrifuged for 5 min. The cytoplasmic fraction was removed, and the nuclear fraction was washed thrice with PBS. Protein was extracted from both fractions using RIPA buffer as described above. The respective supernatants were aspirated, mixed with  $\times 5$  loading buffer (FDbio, cat. FD0006, China) at a ratio of 1:4, and denatured by boiling. An equal amount of protein per sample was separated by 10% sodium dodecyl sulfate polyacrylamide gel electrophoresis and transferred to polyvinylidene fluoride membrane (Millipore, cat. MB0323, United States). After blocking with 10% milk or bovine serum (for phosphorylated proteins), the membranes were incubated overnight with primary antibodies specific for *SMARCC1* (1:500; CST, cat. D7F83, United States), *Cyclin D1* (1:500; CST, cat. 92G2, United States), *Cyclin E1* (1:500; CST, cat. HE12, United States), *CDK6* (1:500; CST, cat. DSC83, United States), *p21* (1:500; CST, cat. 12D1, United States), *p27* (CST, cat. D96C12, United States), *E-Cadherin* (1:500; CST, cat. 24E10/4A2, United States), *N-Cadherin* (1:500; CST, cat. D4R1H, United States), *Vimentin* (1:500; CST, cat. D21H3, United States),  $\beta$ -*catenin* (1:500; CST, cat. D10A8, United States), *Snail* (1:500; CST, cat. C15D3, United States), *Slug* (1:500; CST, cat. C19G7, United States), *Zeb1* (1:500; CST, cat. D80D3, United States), *Zeb2* (1:500; ABclone, cat. A5705, CHINA), *Akt* (1:500; CST, C67E7, United States), *p-Ak<sup>Ser473</sup>* (1:500; CST, cat. D9E, United States), *p-Ak<sup>Thr308</sup>* (1:500; CST, cat. D25E6, United States), *GAPDH* (1:1,000; Proteintech, cat. 104941-AP, China; CST, cat. D4C6R, United States), and *H3* (1:500; Bioss, cat. bs-0349R, China) at 4°C. Total and cytoplasmic proteins were normalized to GAPDH, and nuclear protein was normalized to histone *H3*. PVDF membranes were washed with PBS-tween solution (PBST) and incubated with horseradish peroxidase-conjugated secondary antibody for 1 h. After washing thrice with PBS, the positive bands were detected by FDbio-Dura enhanced chemiluminescence kit (FDbio, cat. FD8020, China).

## Cell Viability Assay

The cells were seeded in 96-well plates at a density of 1,000 cells/well in triplicates, and viability was measured using the Cell Counting Kit 8 (Dojindo, cat. CK04, Japan) according to the manufacturer's instructions. The absorption at

<sup>1</sup><http://gepia.cancer-pku.cn/>



**TABLE 1** | SMARCC1 expression profile in tissue from BPH and PCa.

Origin type of tissue specimens	Immunohistochemical staining intensity		$\chi^2$	P-value
	Negative (n, %)	Positive (n, %)		
BPH	37 (74)	13 (26)	2.487	0.115
PCa	61 (61)	39 (39)		

**TABLE 2** | Correlation between SMARCC1 expression and pathological characteristics of PCa.

Pathological characteristics	Immunohistochemical staining intensity			$\chi^2$	P-value
	Low (n, %)	Medium (n, %)	Strong (n, %)		
<b>Age</b>					
≤60	4 (100)	–	–	2.664	0.264
>60	57 (59.4)	31 (32.3)	8 (8.3)		
<b>Gleason score</b>				<b>7.469</b>	<b>0.024</b>
≤7	27 (50)	23 (42.6)	4 (7.4)		
>7	34 (73.9)	8 (17.4)	4 (8.7)		
<b>T stage</b>				1.547	0.461
T1–2	7 (46.7)	6 (40)	2 (13.3)		
T3–4	50 (63.3)	23 (29.1)	6 (7.6)		
<b>Metastasis to lymph nodes</b>				3.439	0.179
Yes	17 (73.9)	6 (26.1)	–		
No	44 (57.1)	25 (32.5)	8 (10.4)		
<b>Invasion to seminal vesicle</b>				0.375	0.829
Yes	37 (58.7)	21 (33.4)	5 (7.9)		
No	21 (63.6)	9 (27.3)	3 (9.1)		
<b>AJCC clinicopathological stage</b>				3.348	0.501
I–IIc	6 (50)	4 (33.3)	2 (16.7)		
IIIa–IIIc	49 (60.5)	26 (32.1)	6 (7.4)		
IVa–IVb	6 (85.7)	1 (14.3)	0		
<b>ERG staining</b>				3.477	0.176
Negative	37 (63.8)	15 (25.9)	6 (10.3)		
Positive	9 (42.9)	10 (47.6)	2 (9.5)		

Bold values illustrate statistical significance.

450 nm was detected using Microplate Reader Synergy Neo2 (Biotek, United States).

## Colony Formation Assay

The cells were seeded in six-well plates at a density of  $3 \times 10^3$  cells/well in complete medium and cultured for 12–14 days till colonies were visible. The colonies were fixed with methanol and stained using the Wright–Giemsa kit (Baso, cat. BA4017, China). Colonies harboring > 50 cells were counted under a microscope.

## Flow Cytometry Assay

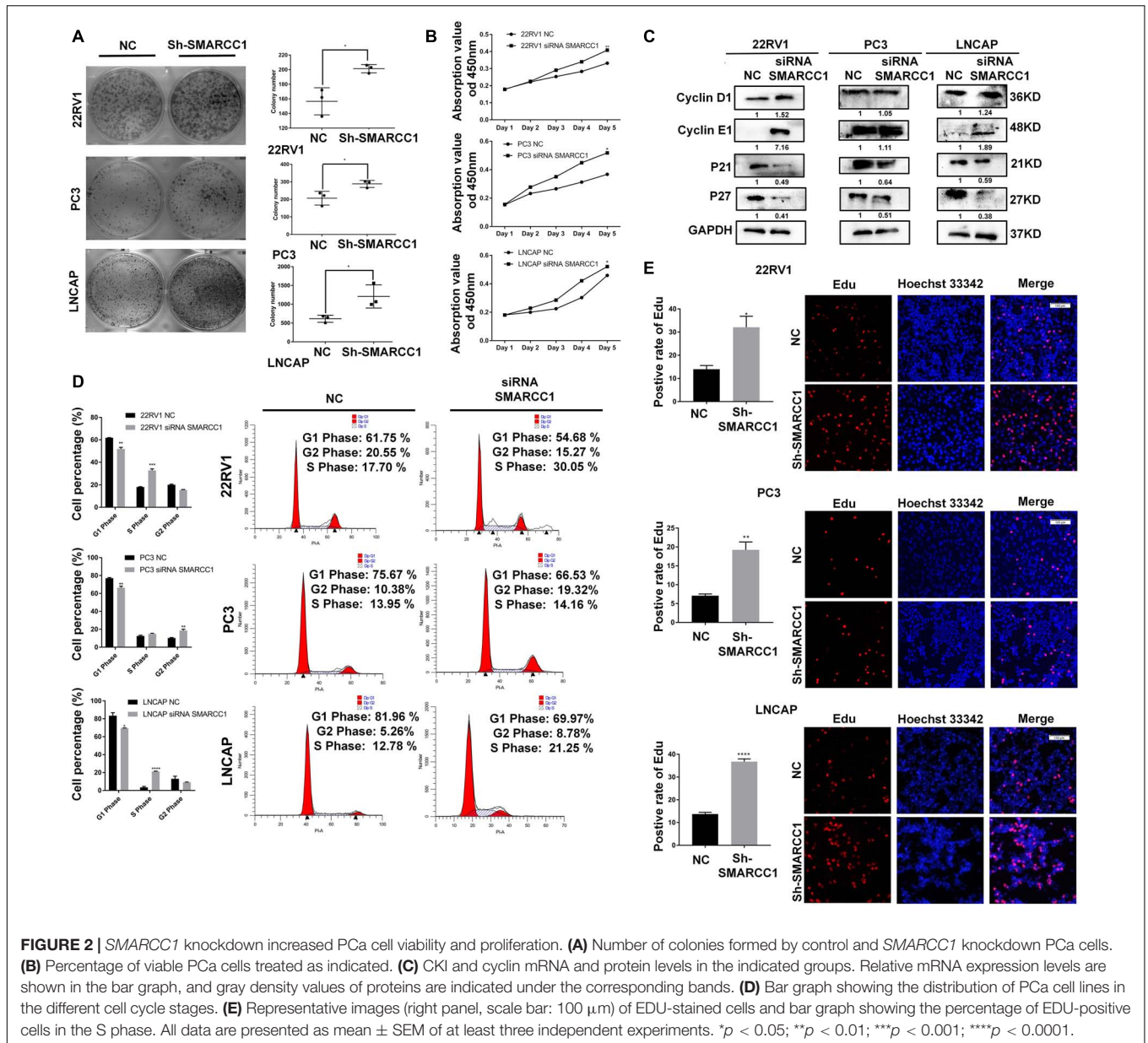
The cell cycle distribution was analyzed using a specific detection kit (KeyGENE BioTECH, cat. KGA512, Nanjing, China). Briefly, the suitably treated cells were harvested and fixed in 75% ethanol for 48 h. After washing with PBS, the cells were incubated with ribonuclease at 37°C for 30 min to remove intracellular RNA. The DNA was stained with propidium iodide (PI), and cells were acquired in the FACS Calibur flow cytometer (Bioscience, United States) to measure the DNA content.

## EDU Assay

The cells were incubated with EDU solution (EDU assay kit, cat. C10310-1, RiboBio, China) diluted 1:1,000 in complete medium for 2 h. After washing thrice with PBS, the cells were fixed with 4% paraformaldehyde for 10 min and neutralized by 2 mg/ml glycine. The cells were then permeabilized with 0.5% Triton and incubated with the kit reaction agent for 30 min. After washing thrice with 0.5% Triton and once with methanol, the cells were counterstained with Hoechst 33342 (diluted 1:1,000 with ddH<sub>2</sub>O) for 10 min to stain the nucleus and washed thrice with PBS. The EDU-positive cells were counted under an inverted microscope (Olympus, cat. 1X71, Japan) fitted with DP72 camera (Olympus, Japan).

## Immunofluorescence Assay

The cells were seeded in a 24-well plate at a density of  $0.2 \times 10^6$  cells/well and fixed with 4% paraformaldehyde for 10 min following 24 h of incubation. After neutralizing with 2 mg/ml glycine, the fixed cells were permeabilized with 0.5% Triton for



10 min and washed thrice with PBS. The cells were then blocked with 10% BSA for 1 h and incubated with primary antibodies against E-Cadherin (1:100; CST, cat. 24E10, United States), N-Cadherin (1:100; CST, cat. D4R1H, United States), Vimentin (1:100; CST, cat. D21H3, United States),  $\beta$ -catenin (1:200; CST, cat. D10A8, United States), and p-Akt<sup>Ser473</sup> (1:200; CST, cat. D9E, United States) at 37°C for 2 h. After washing thrice with PBST for 5 min, the cells were incubated with the secondary antibody at 37°C for 1 h. The stained cells were washed thrice with PBST and observed under an inverted microscope (Olympus, cat. 1X71, Japan) fitted with DP72 camera (Olympus, Japan).

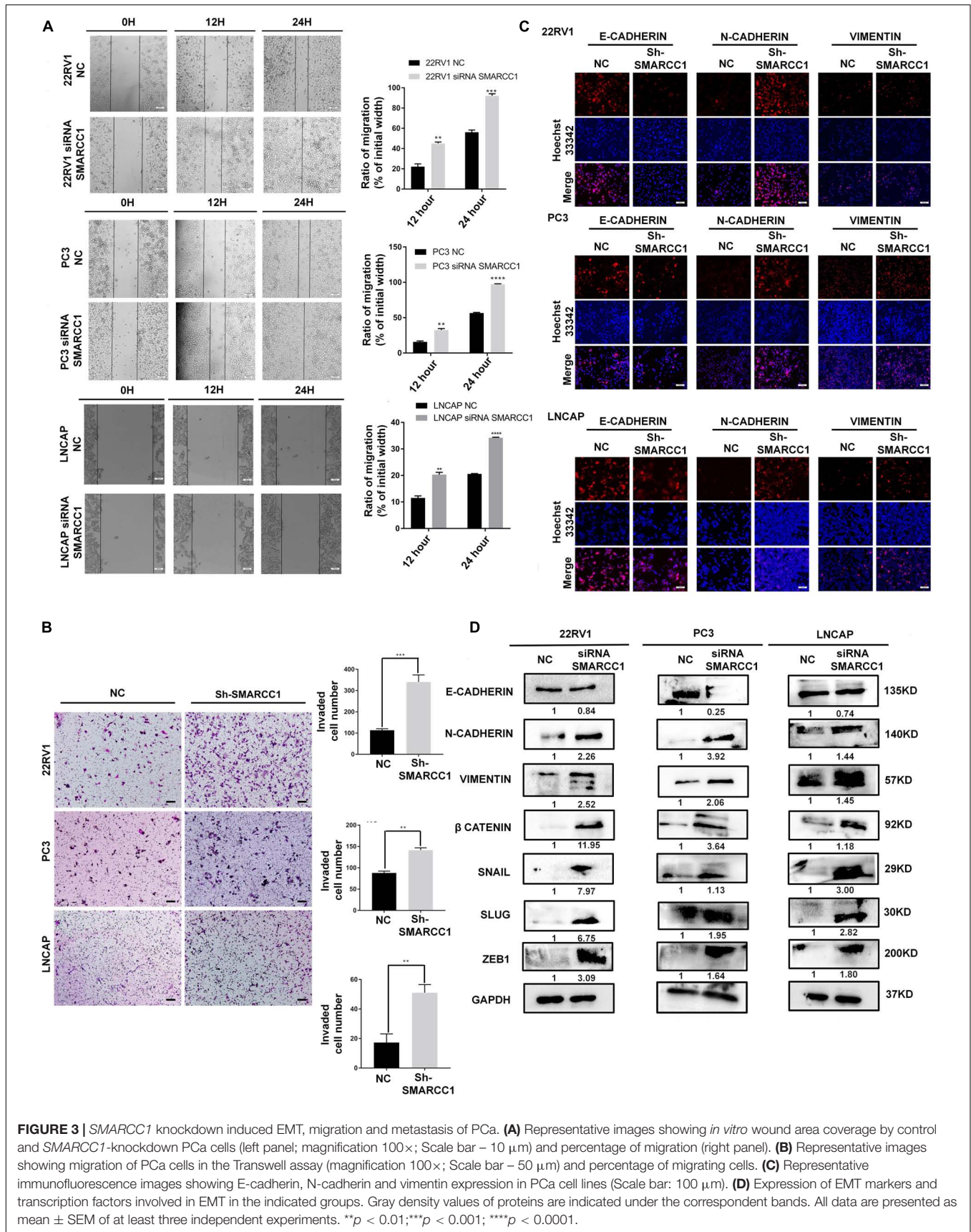
## Wound Healing Assay

The cells were seeded in a six-well plate at a density of  $0.8 \times 10^6$  cells/well and cultured for 48 h till 90% confluent. The monolayer

was scratched longitudinally with a 10- $\mu$ l pipette tip, and the debris was removed by washing thrice with PBS. Fresh serum-free medium was added, and the wound region was photographed at 0, 12, and 24 h after scratching under an inverted microscope (Olympus, cat. 1X71, Japan) with DP72 camera (Olympus, Japan). The extent of wound healing was measured using Image J (NIH, United States).

## Transwell Assay

The cells were seeded in the upper chambers of 24-well Transwell inserts (Corning, cat. 3422, United States) at a density of  $1 \times 10^5$  cells/well in serum-free medium, and the lower chambers were filled with complete medium supplemented with 20% FBS. After culturing for 48 h, the unmigrated cells on the upper surface of the membranes were swabbed



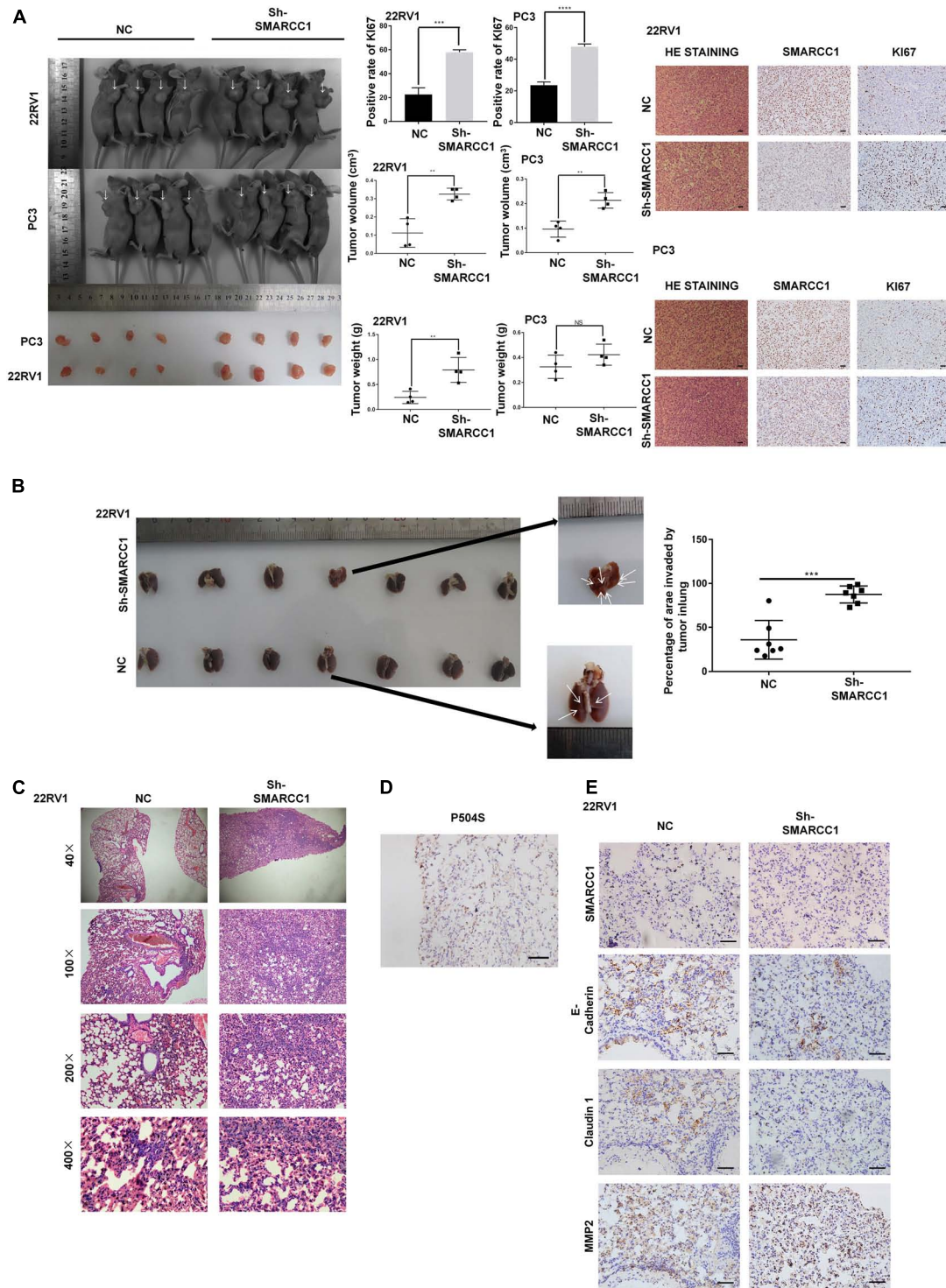


**FIGURE 4 |** *SMARCC1* knockdown promoted tumor growth and metastasis *in vivo*. **(A)** Left panel: representative images of subcutaneous tumor xenografts in the indicated groups and scatter plots showing tumor volume and weight. Right panel: representative immunohistochemistry (IHC) images showing *SMARCC1* and Ki67 expression (magnification,  $\times 200$ ; scale bar,  $20\ \mu\text{m}$ ) and bar graph showing the percentage of Ki67+ cells. **(B,C)** Schematic illustration of lung metastasis model. Representative images of H&E-stained tumor nodules and scatter plots showing the percentage of lung area invaded by PCa cells in the indicated groups. **(D)** Representative IHC images of metastatic nodules showing the positive staining of P504S indicative of prostate origin (magnification,  $\times 400$ ; scale bar,  $20\ \mu\text{m}$ ). **(E)** Representative IHC images of metastatic nodules showing the *in situ* expression of *SMARCC1*, MMP2, E-cadherin, and claudin1 (magnification,  $\times 400$ ; scale bar,  $20\ \mu\text{m}$ ). All data were presented as mean  $\pm$  SEM of at least three independent experiments. \*\* $p < 0.01$ ; \*\*\* $p < 0.001$ ; \*\*\*\* $p < 0.0001$ .

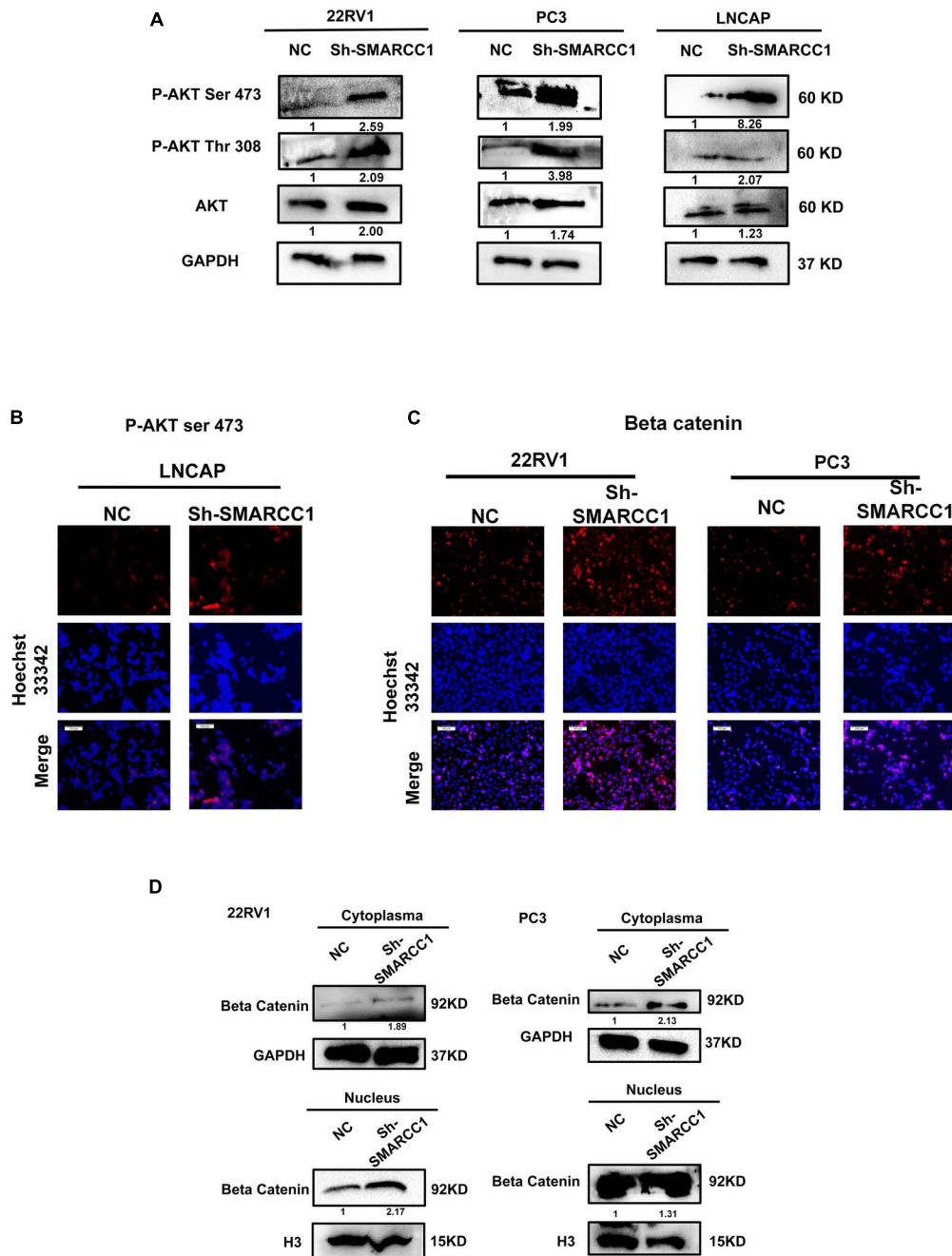


**FIGURE 5 |** SMARCC1 knockdown activated the PI3K/AKT pathway in PCa cell lines. **(A)** Immunoblots showing the expression levels of phosphorylated PI3K/AKT mediators. The gray density values are indicated under the corresponding bands. **(B)** Representative immunofluorescence images showing the *in situ* expression of p-AKT<sup>ser-473</sup> in the LNCAP cell line (scale bar, 100  $\mu$ m). **(C)** Representative immunofluorescence images showing the expression of  $\beta$ -catenin in the cytoplasm and nucleus of 22RV1 and PC3 cell lines (scale bar, 100  $\mu$ m). **(D)** Immunoblots showing the expression levels of  $\beta$ -catenin in the cytoplasmic and nuclear fractions. The gray density values are indicated under the corresponding bands.

with a cotton ball, and the migrated cells on the lower surface were fixed with methanol for 10 min and stained with Wright-Giemsa kit (Baso, cat. BA4017, China). The number of migrated cells were counted in three random fields under a BX53 microscope (Olympus, Japan) fitted with DP72 camera (Olympus, Japan).

## Mouse Xenograft Models

BALB/c nude mice were obtained from Guangdong Medical Laboratory Animal Center (Guangdong, China). All animal experiments were approved by the Ethical Committee of Southern Medical University and conducted according to the

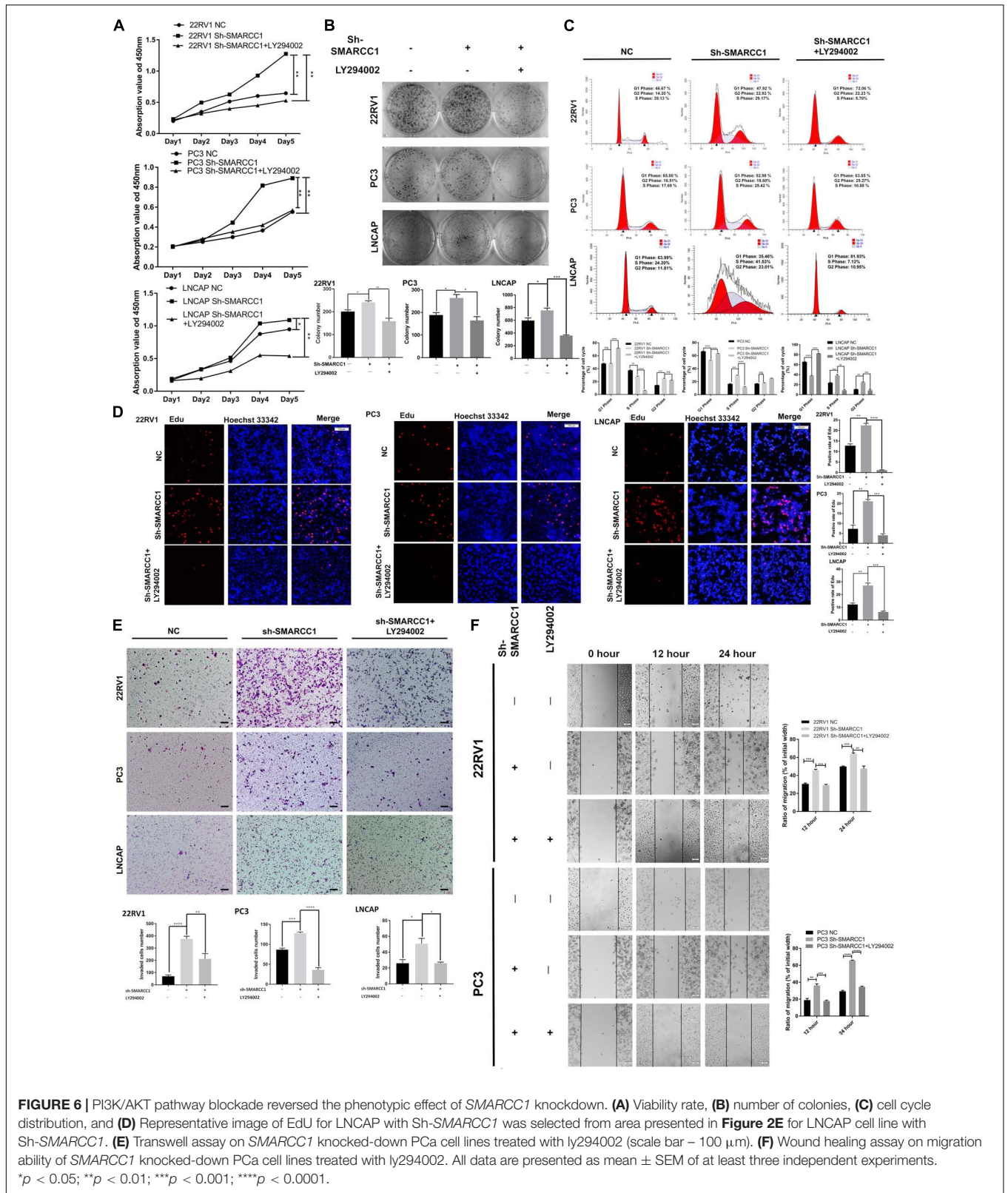
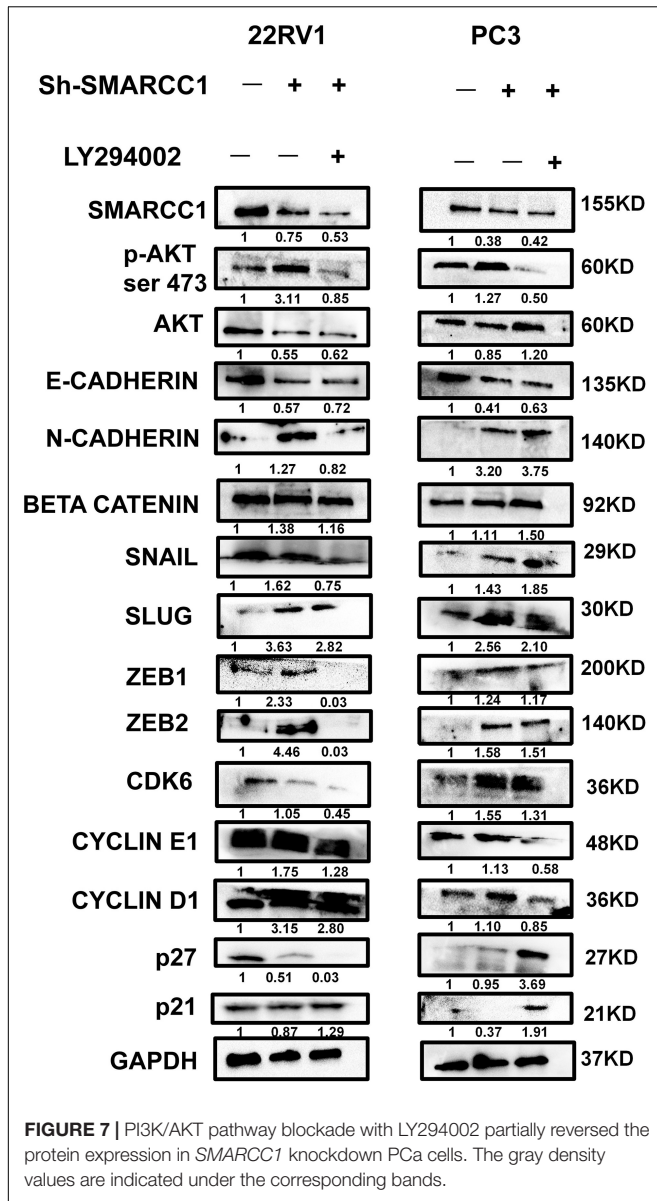


**FIGURE 6** | PI3K/AKT pathway blockade reversed the phenotypic effect of *SMARCC1* knockdown. **(A)** Viability rate, **(B)** number of colonies, **(C)** cell cycle distribution, and **(D)** Representative image of EdU for LNCAP with Sh-SMARCC1 was selected from area presented in **Figure 2E** for LNCAP cell line with Sh-SMARCC1. **(E)** Transwell assay on *SMARCC1* knocked-down Pca cell lines treated with ly294002 (scale bar – 100  $\mu$ m). **(F)** Wound healing assay on migration ability of *SMARCC1* knocked-down Pca cell lines treated with ly294002. All data are presented as mean  $\pm$  SEM of at least three independent experiments. \* $p < 0.05$ ; \*\* $p < 0.01$ ; \*\*\* $p < 0.001$ ; \*\*\*\* $p < 0.0001$ .

NIH Guide for the Care and Use of Laboratory Animals. The subcutaneous xenograft was established in 4-week-old mice by subcutaneously injecting  $5 \times 10^6$  cells into their flanks

(four mice per group). The animals were sacrificed 33 days after inoculation, and the tumors were weighed, measured, and photographed with SX720 HS camera (Canon, Japan). For the



lung metastasis model,  $0.2 \times 10^6$  cells were injected intravenously into 6-week-old mice through the tail vein. The animals were sacrificed 6 weeks later, and the lung tissues were removed and photographed with SX720 HS camera (Canon, Japan). The tissues were fixed in 10% formalin, embedded in paraffin, and cut into sections. Hematoxylin–eosin staining was performed as per standard protocols and photographed under the BX53 microscope (Olympus, Japan) using DP72 camera (Olympus, Japan). IHC was performed to detect the *in situ* expression of proliferation and metastasis markers as described. The area invaded by the tumor was calculated by Image J software (NIH, United States).

## Statistical Analysis

All statistical analyses were performed using GraphPad 7.0 (GraphPad Software Inc., United States) or SPSS 22.0 (IBM

Corp., United States). Chi-square test or Fisher's exact test was used to determine the correlations between the *in situ* protein abundance and the clinicopathological factors in PCa tissues. Numerical data were expressed as means  $\pm$  standard error of mean. Differences between variables were confirmed by two-tailed Student's *t*-test or one-way analysis of variance (ANOVA) for continuous variable groups. When ANOVA was significant, *post-hoc* testing of differences between groups was carried out using the least significant difference test. Survival curves were plotted using Kaplan–Meier's method and compared by the log-rank test. A *P*-value  $< 0.05$  was considered statistically significant.

## RESULTS

### *SMARCC1* Is Downregulated in PCa Tissues With GS More Than 7 and Correlates With Poor Prognosis

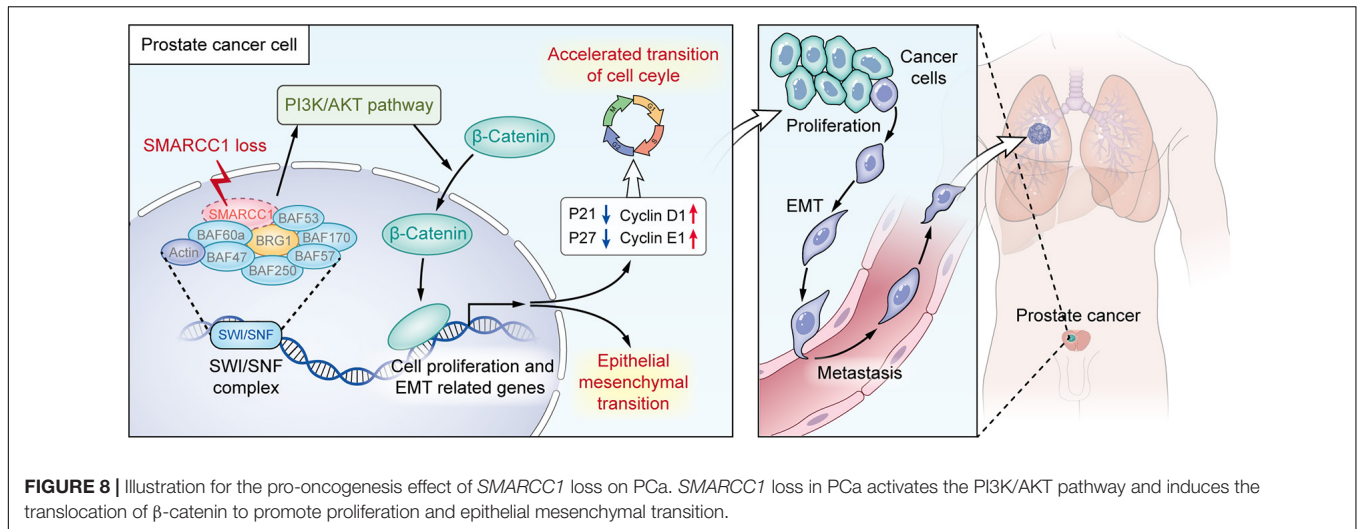
Compared with that in matched non-tumorous tissues of BPH, *in situ SMARCC1* expression in PCa tissue was slightly upregulated without statistical significance (Figure 1A and Table 1). In PCa cases with GS  $> 7$ , *in situ SMARCC1* expression was significantly downregulated (Figure 1A and Table 2). Consistent with this, the GEPIA data showed that the high expression of *SMARCC1* positively correlates with prolonged disease-free survival in PCa patients (Figure 1B). Thus, the loss of *SMARCC1* portends poor prognosis and disease progression in PCa. Moreover, endogenous expression of *SMARCC1* in PCa cell lines was validated using western blotting assay and was further knocked down using transient transfection of siRNA or lentivirus vector containing short hairpin RNA (Figures 1C–E).

### *SMARCC1* Inhibits PCa Cell Proliferation *in vitro*

*SMARCC1* silencing significantly increased the viability of PCa cells as well as the number of colonies formed *in vitro* (Figures 2A,B). Loss of *SMARCC1* upregulated *cyclinD1/E1* and downregulated the *cyclin-dependent kinase inhibitors (CKIs)* *p21* and *p27*, which indicated accelerated cell cycle transition (Figure 2C). Consistent with this, EDU incorporation and PI staining assays showed that *SMARCC1* knockdown increased the percentage of cells entering S and G2 phases and decreased that of cells remaining in G1 phase (Figures 2D,E). In conclusion, *SMARCC1* loss in PCa cells accelerated cell cycle progression and increased their proliferation by downregulating *CKIs* and activating *cyclin D1/E1*.

### *SMARCC1* Silencing Accelerates the Metastasis of PCa Cells by Inducing EMT

Transwell and wound healing assays showed that loss of *SMARCC1* significantly increased the migration of PCa cells *in vitro* (Figures 3A,B). Consistent with this, *SMARCC1* knockdown markedly increased the expression of mesenchymal markers, including vimentin and N-cadherin, and decreased that of *E-cadherin* (Figures 3C,D). In addition, EMT-related transcription factors, including *Slug*, *Snail*, and *Zeb1*, were also



upregulated in the *SMARCC1*-knockdown cells (Figure 3D). In conclusion, *SMARCC1* loss promoted the EMT of PCa cells, thereby inducing migration and metastasis.

### Knockdown of *SMARCC1* Promotes the Growth and Metastasis of Human PCa Cells *in vivo*

To validate the potential impact of *SMARCC1* depletion on PCa cell proliferation *in vivo*, PC-3/sh-*SMARCC1* cells and PC-3/sh-Ctrl as well as 22Rv1/sh-*SMARCC1* cells and 22Rv1/sh-Ctrl cells were injected subcutaneously in nude mice. Tumors in mice implanted with sh-*SMARCC1* cells grew faster than control cells. *SMARCC1* knockdown cells exhibited significantly larger tumor volume and weight than control cells (Figure 4A). H&E staining showed the histopathological features of the tumor tissues. The positive rate of proliferation mark, Ki-67, was dramatically higher in xenografts with sh-*SMARCC1* cells by IHC staining (Figure 4A). These results provided evidence that *SMARCC1* may be a remarkable determinant for PCa cell growth. As for tumor metastasis *in vivo*, a tail vein xenograft model was generated. The tumor presence was validated by histological examination. The results demonstrated that mice injected with 22Rv1/*SMARCC1* shRNA cells produced more lung colonization compared to those with that of the control cells (Figures 4B,C). As shown in Figure 4D, *P540S* was stained to confirm the neoplasms' histologic type and origin of lung colonization. Moreover, we also found that the *SMARCC1*-knockdown pulmonary tumor nodules showed significantly higher levels of the matrix metalloproteinase (MMP2) and low levels of epithelial markers including *E-Cadherin* and *Claudin 1* (Figure 4E).

### Loss of *SMARCC1* Activates the PI3K/AKT Pathway in PCa Cells

*SMARCC1* knockdown activated the PI3K/AKT pathway in PCa cells, as indicated by the elevated phosphorylation of *Akt* at ser-473 and thr-308 (Figures 5A,B). Activation of

the PI3K/AKT pathway stabilizes  $\beta$ -catenin and promotes its nuclear translocation, wherein it regulates the transcription of target genes. Loss of *SMARCC1* significantly increased the accumulation of  $\beta$ -catenin in the nuclear fraction of PCa cells (Figures 5C,D). Furthermore, the PI3K/AKT pathway blockade with the specific inhibitor LY294002 reversed the pro-proliferative and pro-metastatic effects of *SMARCC1* knockdown (Figure 6) without completely altering the expression levels of EMT and proliferation-related factors. This indicates that the PI3K/AKT pathway may partly mediate the pro-oncogenic effect induced by *SMARCC1* knockdown in PCa, and other pathways and mechanisms may also be involved (Figure 7).

## DISCUSSION

High frequent mutations of several key epigenetic factors, including *Rb1* and *BRCA*, have been revealed to induce an aggressive phenotype at the terminal stage of PCa and reflect a promoting effect of epigenetic dysregulation on PCa progression. As one of the core subunits, *SMARCC1* belongs to the SWI/SNF complex, which functions as a key epigenetic complex on genome transcription and consists of 12–14 subunits, including adenosine triphosphatase (ATPase), core, and other accessory subunits (Reisman et al., 2009; Shain and Pollack, 2013; Hohmann and Vakoc, 2014; Alver et al., 2017; Lu and Allis, 2017; Savas and Skardasi, 2018; Lei et al., 2019). A high frequency of mutations with function loss in coding genes of the SWI/SNF complex has been identified by whole genome sequencing in various cancers, especially renal carcinoma and melanoma, implying its important role in tumor suppression (Shain and Pollack, 2013; Stachowiak et al., 2020; Tsuda et al., 2021; Wang et al., 2021; Zhou et al., 2021). Mechanistically, the loss of function of the SWI/SNF complex promotes the transcription of genes related to proliferation and dedifferentiation, impairs DNA repairs, and reduces the antagonistic effect on the PRC complex (Nagl et al., 2005; Wilson et al., 2010; Tolstorukov et al., 2013; Alver et al., 2017; Stanton et al., 2017; Aras et al., 2019; Ribeiro-Silva et al., 2019; Hu et al., 2020).

However, the role of the *SWI/SNF* complex is ambiguous and controversial in PCa (Deocampo et al., 2004; Hong et al., 2005; Link et al., 2005; Heebøll et al., 2008; Hansen et al., 2011; Lee and Roberts, 2013; Prensner et al., 2013). Several studies show that it promotes PCa initiation and progression by transactivating the androgen receptor (Deocampo et al., 2004; Hong et al., 2005; Link et al., 2005), but there are also reports that some subunits function as tumor suppressors (Hansen et al., 2011; Lee and Roberts, 2013; Prensner et al., 2013). For instance, the long non-coding RNA *SchLAPI* promoted an aggressive PCa phenotype by antagonizing the *SNF5* subunit (Lee and Roberts, 2013; Prensner et al., 2013). The effect of *SMARCC1* in PCa is likewise still ambiguous and controversial. One study demonstrated the upregulation of *SMARCC1* in PCa tissues relative to benign prostate tissues (Heebøll et al., 2008), whereas a retrospective study found that the positive staining of *SMARCC1* in PCa tissues correlated with prolonged survival among local PCa patients (Hansen et al., 2011). In this study, we systematically elucidated the expression and role of *SMARCC1* in PCa. Our findings demonstrated that *SMARCC1* was significantly downregulated in PCa tissues with GS > 7, and its low expression correlated with shortened disease-free survival. In addition, silencing of *SMARCC1* in PC-3, 22RV1, and LNCaP cells significantly increased cell proliferation by promoting entry into the S phase of the cell cycle and facilitated cell migration by inducing EMT. The *in vivo* studies using a murine model showed that *SMARCC1* knocking down led to the acceleration of tumor growth and lung metastasis. These observations demonstrated the tumor-suppressive role of *SMARCC1* in PCa.

Infinite proliferation is an important hallmark of tumors (Nagl et al., 2005; Hu et al., 2020). Timing of proliferation depends on the transition speed of cell cycle and is directly associated with the expression of cell cycle-related genes (Nagl et al., 2005; Carrassa, 2013; Hu et al., 2020). Cell cycle transition through different checkpoints is driven by specific cyclins and cyclin-dependent kinases (CDKs) and blocked by CKIs that inhibit cyclins and *cyclin*-CDK complexes (Nagl et al., 2005; Hu et al., 2020). It has been reported that component loss of the *SWI/SNF* complex downregulates CKIs and upregulates cyclins at the transcriptional level (Nagl et al., 2005; Hu et al., 2020). Consistent with previous reports, we found that *SMARCC1* knockdown accelerated cell cycle transition and induced a hyper-proliferative phenotype in PCa cell lines by upregulating G1/S-specific protein *cyclin D1/E1* but downregulating cyclin-dependent kinase inhibitors *p21* and *p27*, implying that *SMARCC1* may be a potential druggable target for cell cycle checkpoint pathway in PCa.

Subunit loss in the *SWI/SNF* complex induces dedifferentiation phenotype, while EMT results from dedifferentiation in cancer cells (Alver et al., 2017; Wang and Unternaehrer, 2019). Previously, studies have indicated that the subunit loss of the *SWI/SNF* complex may facilitate the metastasis of tumor cells by inducing EMT in colon and gastric carcinoma (Yan et al., 2014; Wang et al., 2019). EMT is triggered by transcription factors like *Snail*, *Slug*, and *Zeb1* that repress the epithelial factor *E-cadherin* and

endows the cells with greater metastatic abilities (Yan et al., 2014; Wang and Unternaehrer, 2019; Wang et al., 2019). However, it was uncertain whether the suppression of *SMARCC1* would induce EMT in PCa. We, therefore, analyzed the key proteins of EMT and found that silencing of *SMARCC1* resulted in a remarkably increased expression of vimentin and N-cadherin as well as a reduced expression of E-cadherin, which are considered as characteristic features of EMT.

It has been reported that the component loss in the *SWI/SNF* complex promotes the malignant progression of rhabdomyosarcoma and ovary carcinoma *via* activation of the *PI3K/AKT* pathway (Foster et al., 2009; Bitler et al., 2015). In PCa, activation of the *PI3K/AKT* pathway promotes the nuclear translocation of  $\beta$ -catenin, which triggers the expression of proliferation and EMT-related genes and specifically promotes tumor progression by transactivating androgen receptor and its downstream pathway (Sharma et al., 2002; Hennessy et al., 2005; Carnero, 2010; Noorolyai et al., 2019). However, the specific role of the *PI3K/Akt* pathway in PCa with *SMARCC1* loss still needs to be investigated. Previous studies revealed the synergistic effect of the *SWI/SNF* complex with other epigenetic factors, including histone acetylase and Rb1, on genome transcription (Strobeck et al., 2000; Chatterjee et al., 2018), while *SMARCC1* functions as a scaffold structure in the *SWI/SNF* complex to undertake coordination with other epigenetic factors (Chatterjee et al., 2018), even though we observed a significant upregulation of  $\beta$ -catenin in the nuclear fraction of PCa cells with *SMARCC1* depletion in our study, indicating that the *PI3K/AKT* pathway mediates the pro-oncogenic effects of *SMARCC1* loss. However, the *PI3K/AKT* inhibitor LY294002 only partially reversed these pro-oncogenic effects, which indicates the potential involvement of other epigenetic factors. Taken together, *SMARCC1* may function as a tumor suppressor in PCa along with other epigenetic factors, which warrant further investigation.

In summary, the downregulation of *SMARCC1* is correlated with a poor prognosis and an aggressive phenotype of PCa. *SMARCC1* depletion facilitates PCa cell proliferation by promoting cell cycle progression and enhanced cell migration by EMT. In addition, *SMARCC1* loss activates the *PI3K/Akt* signaling pathway, which plays a key role in the progression of PCa. Therefore, *SMARCC1* may be a promising therapeutic target in PCa, especially for cases with low expression levels (Figure 8).

## DATA AVAILABILITY STATEMENT

The raw data supporting the conclusions of this article will be made available by the authors, without undue reservation.

## ETHICS STATEMENT

The studies involving human participants were reviewed and approved by the Ethics Committee of Nanfang Hospital,

Southern Medical University. The patients/participants provided their written informed consent to participate in this study. The animal study was reviewed and approved by the Ethics Committee of Nanfang Hospital, Southern Medical University.

## AUTHOR CONTRIBUTIONS

Z-MX and D-JL performed the material preparation, data collection, and data analysis. Y-ZY, CW, and TW assisted in collecting data. Z-MX wrote the first draft of the manuscript. D-JL revised the manuscript. S-CZ and D-JL executed the funding acquisition. S-CZ supervised the study. All authors contributed to the study conception and design, commented on previous versions of the manuscript, read, and approved the final manuscript.

## REFERENCES

- Alver, B. H., Kim, K. H., Lu, P., Wang, X., Manchester, H. E., Wang, W., et al. (2017). The SWI/SNF chromatin remodelling complex is required for maintenance of lineage specific enhancers. *Nat. Commun.* 8:14648. doi: 10.1038/ncomms14648
- Andersen, C. L., Christensen, L. L., Thorsen, K., Schepeler, T., Sørensen, F. B., Verspaget, H. W., et al. (2009). Dysregulation of the transcription factors SOX4, CBFβ and SMARCC1 correlates with outcome of colorectal cancer. *Br. J. Cancer* 100, 511–523. doi: 10.1038/sj.bjc.6604884
- Aras, S., Saladi, S. V., Basuroy, T., Marathe, H. G., Lorès, P., and de la Serna, I. L. (2019). BAF60A mediates interactions between the microphthalmia-associated transcription factor and the BRG1-containing SWI/SNF complex during melanocyte differentiation. *J. Cell Physiol.* 234, 11780–11791. doi: 10.1002/jcp.27840
- Bao, J. M., He, M. Y., Liu, Y. W., Lu, Y. J., Hong, Y. Q., Luo, H. H., et al. (2015). AGE/RAGE/Akt pathway contributes to prostate cancer cell proliferation by promoting Rb phosphorylation and degradation. *Am. J. Cancer Res.* 5, 1741–1750.
- Bitler, B. G., Fatkhutdinov, N., and Zhang, R. (2015). Potential therapeutic targets in ARID1A-mutated cancers. *Expert. Opin. Ther. Targets* 19, 1419–1422. doi: 10.1517/14728222.2015.1062879
- Carnero, A. (2010). The PKB/AKT pathway in cancer. *Curr. Pharm. Des.* 16, 34–44. doi: 10.2174/138161210789941865
- Carrassa, L. (2013). Cell cycle, checkpoints and cancer. *Atlas Genet. Cytogenet. Oncol. Haematol.* 18, 67–75.
- Chan, J. J., Kwok, Z. H., Chew, X. H., Zhang, B., Liu, C., Soong, T. W., et al. (2018). A FTH1 gene:pseudogene:miRNA network regulates tumorigenesis in prostate cancer. *Nucleic Acids Res.* 46, 1998–2011. doi: 10.1093/nar/gkx1248
- Chatterjee, S. S., Biswas, M., Boila, L. D., Banerjee, D., and Sengupta, A. (2018). SMARCB1 deficiency integrates epigenetic signals to oncogenic gene expression program maintenance in human acute myeloid leukemia. *Mol. Cancer Res.* 16, 791–804. doi: 10.1158/1541-7786.Mcr-17-0493
- Crea, F., Hurt, E. M., Mathews, L. A., Cabarcas, S. M., Sun, L., Marquez, V. E., et al. (2011). Pharmacologic disruption of Polycomb Repressive Complex 2 inhibits tumorigenicity and tumor progression in prostate cancer. *Mol. Cancer* 10, 40. doi: 10.1186/1476-4598-10-40
- Deocampo, N. D., Bello-Deocampo, D., and Tindall, D. J. (2004). SWI/SNF as an enhancer of androgen receptor transactivation in prostate cells. *Cancer Res.* 64, 840–840.
- Foster, K., Wang, Y., Zhou, D., and Wright, C. (2009). Dependence on PI3K/Akt signaling for malignant rhabdoid tumor cell survival. *Cancer Chemother. Pharmacol.* 63, 783–791. doi: 10.1007/s00280-008-0796-5

## FUNDING

This study was supported by the National Natural Science Foundation of China (No. 81972394), the Guangdong Basic and Applied Basic Research Foundation (2020A1515010066), the Outstanding Youths Development Scheme of Nanfang Hospital, Southern Medical University (No. 2015J005), the China Postdoctoral Science Foundation funded project (No. 2019M662865), the Guangdong Basic and Applied Basic Research Foundation (No. 2019A1515110033), the Distinguished Young Talents in Higher Education Foundation of Guangdong Province (No. 2019KQNCX115), the Achievement Cultivation and Clinical Transformation Application Cultivation projects of the First Affiliated Hospital of Guangzhou Medical University (No. ZH201908), and the Science and Technology Plan Project of Guangzhou (No. 202102010150).

- Ge, R., Wang, Z., Montironi, R., Jiang, Z., Cheng, M., Santoni, M., et al. (2020). Epigenetic modulations and lineage plasticity in advanced prostate cancer. *Ann. Oncol.* 31, 470–479. doi: 10.1016/j.annonc.2020.02.002
- Hansen, R. L., Heebøll, S., Ottosen, P. D., Dyrskjøt, L., and Borre, M. (2011). Smarcc1 expression: a significant predictor of disease-specific survival in patients with clinically localized prostate cancer treated with no intention to cure. *Scand. J. Urol. Nephrol.* 45, 91–96. doi: 10.3109/00365599.2010.530295
- Heebøll, S., Borre, M., Ottosen, P. D., Andersen, C. L., Mansilla, F., Dyrskjøt, L., et al. (2008). SMARCC1 expression is upregulated in prostate cancer and positively correlated with tumour recurrence and dedifferentiation. *Histol. Histopathol.* 23, 1069–1076. doi: 10.14670/hh-23.1069
- Hennessy, B. T., Smith, D. L., Ram, P. T., Lu, Y., and Mills, G. B. (2005). Exploiting the PI3K/AKT pathway for cancer drug discovery. *Nat. Rev. Drug Discov.* 4, 988–1004. doi: 10.1038/nrd1902
- Hohmann, A. F., and Vakoc, C. R. (2014). A rationale to target the SWI/SNF complex for cancer therapy. *Trends Genet.* 30, 356–363. doi: 10.1016/j.tig.2014.05.001
- Hong, C. Y., Suh, J. H., Kim, K., Gong, E. Y., Jeon, S. H., Ko, M., et al. (2005). Modulation of androgen receptor transactivation by the SWI3-related gene product (SRG3) in multiple ways. *Mol. Cell Biol.* 25, 4841–4852. doi: 10.1128/mcb.25.12.4841-4852.2005
- Hu, B., Lin, J. Z., Yang, X. B., and Sang, X. T. (2020). The roles of mutated SWI/SNF complexes in the initiation and development of hepatocellular carcinoma and its regulatory effect on the immune system: a review. *Cell Prolif.* 53:e12791. doi: 10.1111/cpr.12791
- Iwagami, Y., Eguchi, H., Nagano, H., Akita, H., Hama, N., Wada, H., et al. (2013). miR-320c regulates gemcitabine-resistance in pancreatic cancer via SMARCC1. *Br. J. Cancer* 109, 502–511. doi: 10.1038/bjc.2013.320
- Lee, R. S., and Roberts, C. W. (2013). Linking the SWI/SNF complex to prostate cancer. *Nat. Genet.* 45, 1268–1269. doi: 10.1038/ng.2805
- Lei, I., Tian, S., Chen, V., Zhao, Y., and Wang, Z. (2019). SWI/SNF component BAF250a coordinates OCT4 and WNT signaling pathway to control cardiac lineage differentiation. *Front. Cell Dev. Biol.* 7:358. doi: 10.3389/fcell.2019.00358
- Liang, C., Niu, L., Xiao, Z., Zheng, C., Shen, Y., Shi, Y., et al. (2020). Whole-genome sequencing of prostate cancer reveals novel mutation-driven processes and molecular subgroups. *Life Sci.* 254:117218. doi: 10.1016/j.lfs.2019.117218
- Link, K. A., Burd, C. J., Williams, E., Marshall, T., Rosson, G., Henry, E., et al. (2005). BAF57 governs androgen receptor action and androgen-dependent proliferation through SWI/SNF. *Mol. Cell Biol.* 25, 2200–2215. doi: 10.1128/mcb.25.6.2200-2215.2005
- Liu, W. (2016). DNA alterations in the tumor genome and their associations with clinical outcome in prostate cancer. *Asian J. Androl.* 18, 533–542. doi: 10.4103/1008-682x.177120

- Lu, C., and Allis, C. D. (2017). SWI/SNF complex in cancer. *Nat. Genet.* 49, 178–179. doi: 10.1038/ng.3779
- Nagl, N. G. Jr., Patsialou, A., Haines, D. S., Dallas, P. B., Beck, G. R. Jr., and Moran, E. (2005). The p270 (ARID1A/SMARCF1) subunit of mammalian SWI/SNF-related complexes is essential for normal cell cycle arrest. *Cancer Res.* 65, 9236–9244. doi: 10.1158/0008-5472.Can-05-1225
- Noorolyai, S., Shajari, N., Baghbani, E., Sadreddini, S., and Baradaran, B. (2019). The relation between PI3K/AKT signalling pathway and cancer. *Gene* 698, 120–128. doi: 10.1016/j.gene.2019.02.076
- Oh, M., Alkushaym, N., Fallatah, S., Althagafi, A., Aljaded, R., Alswaida, Y., et al. (2019). The association of BRCA1 and BRCA2 mutations with prostate cancer risk, frequency, and mortality: a meta-analysis. *Prostate* 79, 880–895. doi: 10.1002/pros.23795
- Pernar, C. H., Ebot, E. M., Wilson, K. M., and Mucci, L. A. (2018). The epidemiology of prostate cancer. *Cold Spring Harb. Perspect. Med.* 8:a030361. doi: 10.1101/cshperspect.a030361
- Prensner, J. R., Iyer, M. K., Sahu, A., Asangani, I. A., Cao, Q., Patel, L., et al. (2013). The long noncoding RNA SchLAP1 promotes aggressive prostate cancer and antagonizes the SWI/SNF complex. *Nat. Genet.* 45, 1392–1398. doi: 10.1038/ng.2771
- Reisman, D., Glaros, S., and Thompson, E. A. (2009). The SWI/SNF complex and cancer. *Oncogene* 28, 1653–1668. doi: 10.1038/onc.2009.4
- Ribeiro-Silva, C., Vermeulen, W., and Lans, H. (2019). SWI/SNF: complex complexes in genome stability and cancer. *DNA Rep. (Amst)* 77, 87–95. doi: 10.1016/j.dnarep.2019.03.007
- Savas, S., and Skardasi, G. (2018). The SWI/SNF complex subunit genes: their functions, variations, and links to risk and survival outcomes in human cancers. *Crit. Rev. Oncol. Hematol.* 123, 114–131. doi: 10.1016/j.critrevonc.2018.01.009
- Shain, A. H., and Pollack, J. R. (2013). The spectrum of SWI/SNF mutations, ubiquitous in human cancers. *PLoS One* 8:e55119. doi: 10.1371/journal.pone.0055119
- Sharma, M., Chuang, W. W., and Sun, Z. (2002). Phosphatidylinositol 3-kinase/Akt stimulates androgen pathway through GSK3beta inhibition and nuclear beta-catenin accumulation. *J. Biol. Chem.* 277, 30935–30941. doi: 10.1074/jbc.M201919200
- Sheahan, A. V., and Ellis, L. (2018). Epigenetic reprogramming: a key mechanism driving therapeutic resistance. *Urol. Oncol.* 36, 375–379. doi: 10.1016/j.urolonc.2017.12.021
- Siegel, R. L., Miller, K. D., Fuchs, H. E., and Jemal, A. (2021). Cancer statistics, 2021. *CA Cancer J. Clin.* 71, 7–33. doi: 10.3322/caac.21654
- Stachowiak, M., Szymanski, M., Ornoch, A., Jancewicz, I., Rusetska, N., Chrzan, A., et al. (2020). SWI/SNF chromatin remodeling complex and glucose metabolism are deregulated in advanced bladder cancer. *IUBMB Life* 72, 1175–1188. doi: 10.1002/iub.2254
- Stanton, B. Z., Hodges, C., Calarco, J. P., Braun, S. M., Ku, W. L., Kadoch, C., et al. (2017). Smarca4 ATPase mutations disrupt direct eviction of PRC1 from chromatin. *Nat. Genet.* 49, 282–288. doi: 10.1038/ng.3735
- Strobeck, M. W., Knudsen, K. E., Fribourg, A. F., DeCristofaro, M. F., Weissman, B. E., Imbalzano, A. N., et al. (2000). BRG-1 is required for RB-mediated cell cycle arrest. *Proc. Natl. Acad. Sci. U.S.A.* 97, 7748–7753. doi: 10.1073/pnas.97.14.7748
- Tolstorukov, M. Y., Sansam, C. G., Lu, P., Koellhoffer, E. C., Helming, K. C., Alver, B. H., et al. (2013). Swi/Snf chromatin remodeling/tumor suppressor complex establishes nucleosome occupancy at target promoters. *Proc. Natl. Acad. Sci. U.S.A.* 110, 10165–10170. doi: 10.1073/pnas.1302209110
- Tsuda, M., Fukuda, A., Kawai, M., Araki, O., and Seno, H. (2021). The role of the SWI/SNF chromatin remodeling complex in pancreatic ductal adenocarcinoma. *Cancer Sci.* 112, 490–497. doi: 10.1111/cas.14768
- Wang, G., Lv, Q., Ma, C., Zhang, Y., Li, H., and Ding, Q. (2021). SMARCC1 expression is positively correlated with pathological grade and good prognosis in renal cell carcinoma. *Transl. Androl. Urol.* 10, 236–242. doi: 10.21037/tau-20-935
- Wang, H., and Unternaehrer, J. J. (2019). Epithelial-mesenchymal transition and cancer stem cells: at the crossroads of differentiation and dedifferentiation. *Dev. Dyn.* 248, 10–20. doi: 10.1002/dvdy.24678
- Wang, W., Friedland, S. C., Guo, B., O'Dell, M. R., Alexander, W. B., Whitney-Miller, C. L., et al. (2019). ARID1A, a SWI/SNF subunit, is critical to acinar cell homeostasis and regeneration and is a barrier to transformation and epithelial-mesenchymal transition in the pancreas. *Gut* 68, 1245–1258. doi: 10.1136/gutjnl-2017-315541
- Wilson, B. G., Wang, X., Shen, X., McKenna, E. S., Lemieux, M. E., Cho, Y. J., et al. (2010). Epigenetic antagonism between polycomb and SWI/SNF complexes during oncogenic transformation. *Cancer Cell* 18, 316–328. doi: 10.1016/j.ccr.2010.09.006
- Wu, G., Sun, Y., Xiang, Z., Wang, K., Liu, B., Xiao, G., et al. (2019). Preclinical study using circular RNA 17 and micro RNA 181c-5p to suppress the enzalutamide-resistant prostate cancer progression. *Cell Death Dis.* 10:37. doi: 10.1038/s41419-018-1048-1
- Yan, H. B., Wang, X. F., Zhang, Q., Tang, Z. Q., Jiang, Y. H., Fan, H. Z., et al. (2014). Reduced expression of the chromatin remodeling gene ARID1A enhances gastric cancer cell migration and invasion via downregulation of E-cadherin transcription. *Carcinogenesis* 35, 867–876. doi: 10.1093/carcin/bgt398
- Zhou, M., Yuan, J., Deng, Y., Fan, X., and Shen, J. (2021). Emerging role of SWI/SNF complex deficiency as a target of immune checkpoint blockade in human cancers. *Oncogenesis* 10:3. doi: 10.1038/s41389-020-00296-6

**Conflict of Interest:** The authors declare that the research was conducted in the absence of any commercial or financial relationships that could be construed as a potential conflict of interest.

Copyright © 2021 Xiao, Lv, Yu, Wang, Xie, Wang, Song and Zhao. This is an open-access article distributed under the terms of the Creative Commons Attribution License (CC BY). The use, distribution or reproduction in other forums is permitted, provided the original author(s) and the copyright owner(s) are credited and that the original publication in this journal is cited, in accordance with accepted academic practice. No use, distribution or reproduction is permitted which does not comply with these terms.